Behavioral changes preceded by subthalamic nucleus alterations in a progressive macaque model of Parkinson's disease.

Bertrand, Mathilde PhD[1], Hugues Dit Ciles, Jessy[1], Chabardes, Stephan PhD, MD[1-2-3], De Leiris, Nicolas PhD[4], Baudin, Bruno PhD, MD[5], Bastin, Julien PhD[1], Piallat, Brigitte PhD[1,*]

1. Univ. Grenoble Alpes, Inserm, U1216, Grenoble Institute of Neurosciences, 38000 Grenoble, France
2. Univ. Grenoble Alpes, Department of Neurosurgery, Inserm, U1216, CHU Grenoble Alpes, Grenoble Institute Neurosciences, 38000 Grenoble, France
3. Clinatec-CEA Leti, 38000 Grenoble, France
4. UMR Inserm, 1039, Department of Nuclear Medecine, University Hospital of Grenoble Alpes, 38000 Grenoble, France
5. Univ. Paris-Saclay, Inserm, U1193, 91400 Orsay, France and Biochemistry Laboratory, Armand Trousseau Hospital, 75571 Paris, France

* Corresponding author: Brigitte.piallat@univ-grenoble-alpes.fr

ABSTRACT

Parkinson's disease (PD) is diagnosed after motor symptoms appear, although non-motor symptoms emerge years earlier. Following years of pharmacological treatment, high-frequency stimulation (HFS) of the subthalamic nucleus (STN), a key hub in goal-direct behaviors, can be proposed. While HFS-STN reliably improves motor symptoms, it does not specifically address non-motor symptoms. Clarifying how STN dysfunction contributes to non-motor symptoms could thus improve STN stimulation strategies. Here, we longitudinally recorded STN local field potentials in two macaques performing a counter-demanding task during chronic low-dose MPTP treatment. This progressive model, evolving from an asymptomatic stage to motivational, cognitive and ultimately motor deficits, enabled detailed examination of non-motor stages preceding motor impairment. Each stage was associated with distinct STN electrophysiological alterations, including early loss of reward-related theta activity, subsequent disappearance of decision-related theta oscillations, and later reduction of movement-related beta rebound. In the stable parkinsonian stage, stimulation of different STN territories provided complementary behavioral effect: dorsal HFS-STN improved motor performances, whereas ventral low-frequency stimulation alleviated motivational deficits. These findings reveal a temporal link between STN dysfunction and symptom onset, and suggest site and frequency-specific stimulation as a strategy to address both motor and non-motor symptoms in PD.

INTRODUCTION

Parkinson's disease (PD) is a progressive neurodegenerative disorder characterized not only by cardinal motor symptoms but also by a range of non-motor symptoms, including sleep/wake disturbances, apathy, and cognitive decline, which precede motor signs by years[1–3]. Understanding the neural substrates of these early manifestations is critical for enabling early diagnosis and developing targeted therapies[4]. The subthalamic nucleus (STN) is a central hub in the basal ganglia-thalamo-cortical network, integrating cortical inputs to shape and adapt goal-directed behaviors[5,6]. In PD, pathological STN beta-band activity (12-35 Hz) is associated with motor symptoms occurrence and abolished by dorsolateral STN high-frequency stimulation (HFS, ~130 Hz), which improves motor symptoms[7–10]. Beyond motor control, accumulating evidence implicates STN theta-band (4-8 Hz) alterations with non-motor PD symptoms, including impaired conflict resolution, apathy, impulsivity, and depression[11–15].

We recently demonstrated correlations between physiological STN activity and distinct behavioral domains in non-human primate (NHP), providing a framework for studying how these dynamics progress during PD[16]. Among available preclinical models, the NHP parkinsonian model induced by 1-methyl-4-phenyl-1,2,3,6-tetrahydropyridine (MPTP) remains the gold standard, as it reproduces both motor and non-motor impairments alongside nigro-striatal degeneration[17–19]. In particular, chronic low-dose MPTP treatment induces a progressive PD phenotype[20,21] enabling longitudinal study of STN activity and its temporal relationship to the onset of non-motor and motor manifestations.

Deep brain stimulation (DBS) provides a causal approach to explore STN functions. While HFS of the dorsolateral STN reliably alleviates motor symptoms, it can exacerbate non-motor impairments[22,23]. Conversely, dorsal low-frequency stimulation (LFS, ~4-5 Hz) has shown promise for improving non-motor symptoms in PD patients, including deficits in conflict resolution and impulsivity, likely by engaging prefrontal-STN hyperdirect pathway[24–26]. With emerging adaptive DBS technologies enabling site and frequency-specific modulation[27–30], clarifying the temporal and functional dynamics of STN alterations has become a pressing clinical priority.

Here, we investigated the time-based longitudinal relationship between STN activity and the sequential emergence of motivational, cognitive, and motor deficits in a progressive NHP model of PD. We reveal that STN alterations precede behavioral changes, with theta disruptions related to motivational and cognitive deficits, and abnormal beta activity associated with motor symptoms. In a stable parkinsonian syndrome, we further demonstrate site and

frequency-specific STN stimulation effects, with dorsal HFS improving motor impairments and ventral LFS alleviating motivational deficits.

RESULTS

Progressive parkinsonian syndrome

Chronic low-dose MPTP administration (0.2-0.5 mg/kg, biweekly) induced a progressive parkinsonian syndrome in both monkeys. M1 received 20 injections (5.45 mg/kg over 43 weeks) and M2 received 18 injections (6.7 mg/kg over 39 weeks), and both reached a similar stable moderate parkinsonian syndrome. Using a validated scale to evaluate motor manifestations[31], we identified three severity stages (**Fig. 1A**): stage 1 (score 0-3), asymptomatic, with no motor signs; stage 2 (score 4-10), mild parkinsonism, with light and unstable deficits; and stage 3 (score >10), moderate parkinsonism, with significant and stable motor manifestations, including reduced activity, bradykinesia, and flexed posture.

Longitudinal DaT SPECT imaging revealed a progressive decrease in striatal Ioflupane tracer relative to the occipital cortex, beginning after the first MPTP injection (**Fig. 1B**). Both monkeys developed similar trajectories, except for a transient increase during stage 2 for M1, which led to a closer behavioral examination during this stage.

Finally, we analyzed serial cerebrospinal fluid (CSF) to identify metabolite correlates of the dopaminergic deficit (**Fig. 1C**). In both monkeys, homovanillic acid (HVA), principal dopamine metabolite, progressively decrease and 3-methoxy-4-hydroxyphenylglycol (MHPG), major noradrenaline metabolite, was significantly reduced from stage 1. M1 also showed a progressive decrease in 5-hydroxy indoleacetic acid (5-HIAA), main serotonin metabolite, whereas 3-ortho-methyldopa (3-OMD), product of dopamine synthesis, remained unchanged.

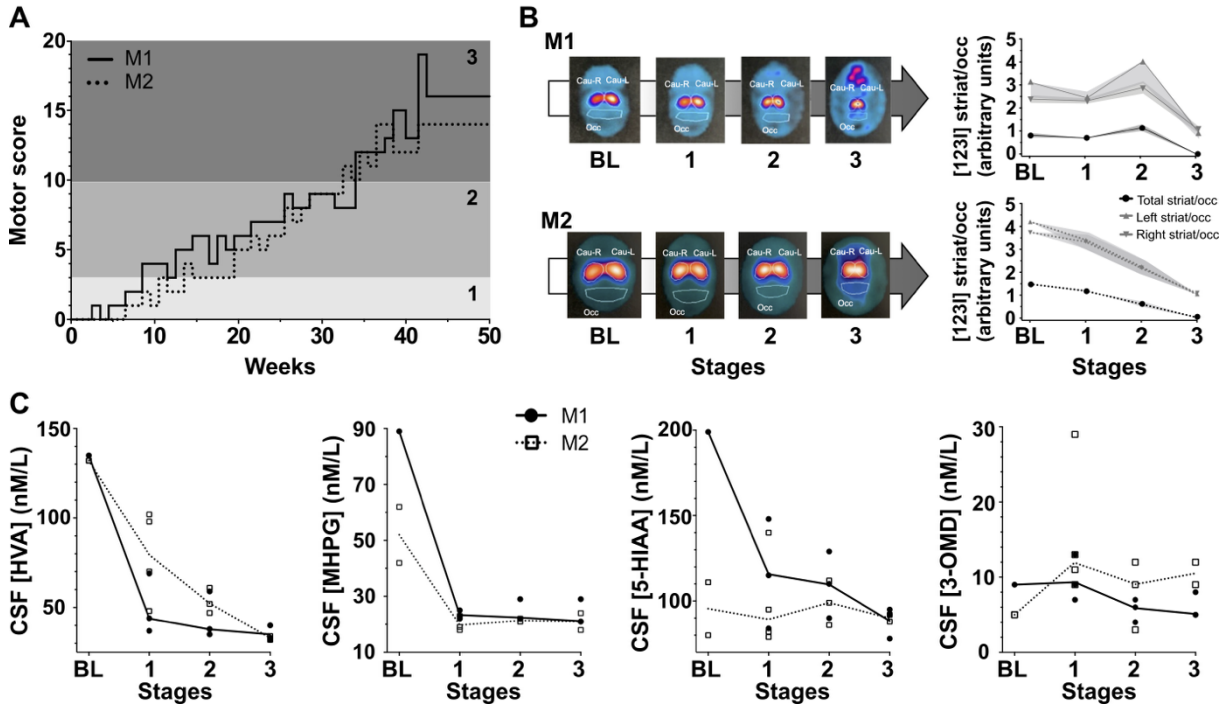

Figure 1: Progressive parkinsonian syndrome for M1 (solid line) and M2 (dotted line). (A) Weekly evaluation of the parkinsonian syndrome induced by chronic low-dose MPTP administration. Motor score discriminated 3 stages: 1-asymptomatic (very light gray, score 0-3); 2-mild parkinsonism (light gray, score 4-10); 3-moderate parkinsonism (dark gray, score >10). **(B)** DaT SPECT imaging using Ioflupane (I^{123}) tracer for each stage with ratios quantification between the left and right striatum (Cau-L and Cau-R) relative to cerebral background noise (Occ). **(C)** Lumbar cerebrospinal fluid (CSF) concentrations of homovanillic acid (HVA), 5-hydroxyindole acetic acid (5-HIAA), 3-methoxy-4-hydroxyphenylglycol (MHPG), and 3-ortho-methyldopa (3-OMD). BL, baseline before MPTP treatment.

Early non-motor manifestations

Before and during MPTP treatment, both monkeys performed a validated counter-demanding task discriminating motivational, cognitive and motor behaviors[16]. On each trial, they could either perform a switching task (Work), where correct responses filled a gauge, or checked the gauge itself (Check) to monitor their progress toward a bonus reward delivered once full (**Fig. 2A**, see methods). Motivation was assessed by the probability to check when the gauge was full (Reward Check); cognitive performance by the error rate on Switch trials (Error Switch) and Switch-Cost (response time difference between correct Switch and Non-Switch trials); and motor performance by response time on correct Non-Switch trials (mRT). Each monkey completed at least five sessions per stage (≥4 bonus rewards/session; **Supplemental Table 1**): M1 performed 10, 17, 13, 6 and 6 sessions at baseline, stage 1, stage 2, stage 2', and stage 3, respectively; and M2 performed 10, 16, 9, 7, and 5 sessions.

During stage 1, just after starting MPTP treatment, no significant behavioral effects were found for both monkeys, consistent with an asymptomatic stage.

In stage 2, non-motor signs appeared in a specific chronology, distinguishing two substages: early stage 2, affecting motivation with decreased Check Reward medians (for **M1-** BL: 28% (IQR 23-32) vs. stage 2: 21% (17-23), p=0.039; for **M2-** BL: 23% (21-27) vs. stage 2: 15% (14-16), p=0.010) (**Fig. 2B**); and late stage 2', affecting cognitive behavior with increased Switch Error (for **M1-** BL: 2.8% (2.7-3) vs. stage 2': 6.4% (6-6.6), p<0.001; for **M2-** BL: 6.0% (5.5-7) vs. stage 2': 8.1% (7.8-8.8), p<0.001) (**Fig. 2C**). M2 also exhibited a mean negative Switch-Cost (BL: 45.1 ± 4.4ms vs. stage 2': -3.9 ± 5.7ms, p<0.001), suggesting advanced cognitive impairment (**Fig. 2D**).

Finally, during stage 3, both monkeys displayed slower motor response time with increased mRT (for **M1-** BL: 411ms (IQR 372-478) vs. stage 3: 501ms (460-603), p<0.001; for **M2-** BL: 454ms (390-536) vs. stage 3: 487ms (399-676), p<0.001) (**Fig. 2E**).

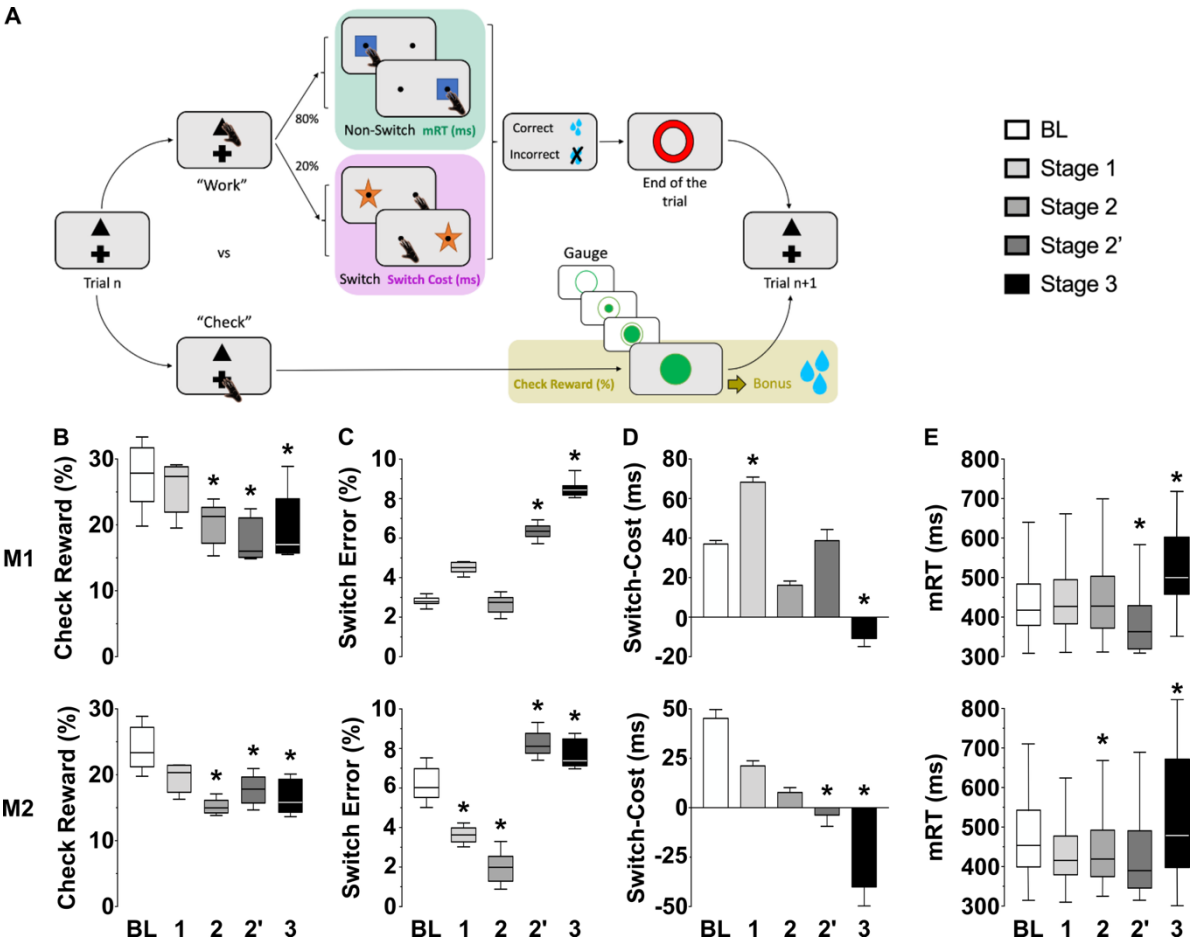

Figure 2: Behavioral effect of MPTP treatment across stages. **(A)** Rewarded task assessing limbic (gold), cognitive (pink), and motor (green) behaviors. On each trial, monkeys decided to "Work" on the main switching task, or "Check" the size of a gauge indicating the proximity of a bonus reward (see Methods). **(B)** Probabilities to check when the reward is available (Check Reward, %). **(C)** Errors on Switch trials (Switch Error, %). **(D)** Switch-Cost in ms, response time difference between Switch and Non-Switch trials. **(E)** Motor response time (mRT, ms) on Non-Switch trials. Stages: baseline, before MPTP treatment (BL, white); stage 1, asymptomatic (1, very light gray); early stage 2, mild parkinsonism (2, light gray); late stage 2', mild parkinsonism (2', light gray), stage 3, moderate parkinsonism (3, dark

gray). The horizontal line represents the median, except for Switch-Cost (mean ± SEM). *p<0.05, Kruskal-Wallis followed by Dunn's multiple comparisons test.

Evolution of STN activity

STN local field potentials were recorded while monkeys performed the behavioral task at baseline and throughout MPTP treatment. Time-frequency representations of spectral power were averaged across trials within each condition and aligned to task events. Band-specific powers within defined time windows were then quantified and compared across stages.

During reward delivery, baseline activity showed a significant decrease in theta oscillations (4-8Hz) for both monkeys ($p<0.05$, two-sample t-test) (**Fig. 3A**). This decreased theta disappeared, starting from stage 1, with theta power significantly higher at all parkinsonian stages compared to baseline (for **M1-** BL: -3.4 ± 0.2LdB vs. stage 1: 1.3 ± 0.1 LdB, $p<0.001$; for **M2-** BL: -2.2 ± 0.1LdB vs. stage 1: 0.5 ± 0.2LdB, $p<0.001$).

When monkeys chose to work rather than check, baseline activity showed a significant increase in theta oscillations for both monkeys ($p<0.05$, two-sample t-test) (**Fig. 3B**). This effect was preserved in stage 1 but disappeared from early stage 2, with theta power significantly lower than baseline (for **M1-** BL: 0.9 ± 0.1LdB vs. stage 2: -0.1 ± 0.1LdB, $p<0.001$; for **M2-** BL: 1.5 ± 0.1LdB vs. stage 2: 0.1 ± 0.1LdB, $p=0.004$).

At the onset of the motor cue, baseline activity showed a significant decrease in beta oscillations followed by a rebound beta increase for both monkeys ($p<0.05$, one-sample t-test) (**Fig. 3C**). This rebound persisted during stage 1 and early stage 2 but disappeared from stage 2'. Quantification of beta rebound confirmed significant reductions at stage 2' for M1 and at stage 3 for M2 (for **M1-** BL: 5.0 ± 0.1LdB vs. stage 2': 0.5 ± 0.3LdB, $p<0.001$; for **M2-** BL: 1.0 ± 0.1% vs. stage 3: -1.8 ± 0.1LdB, $p=0.021$).

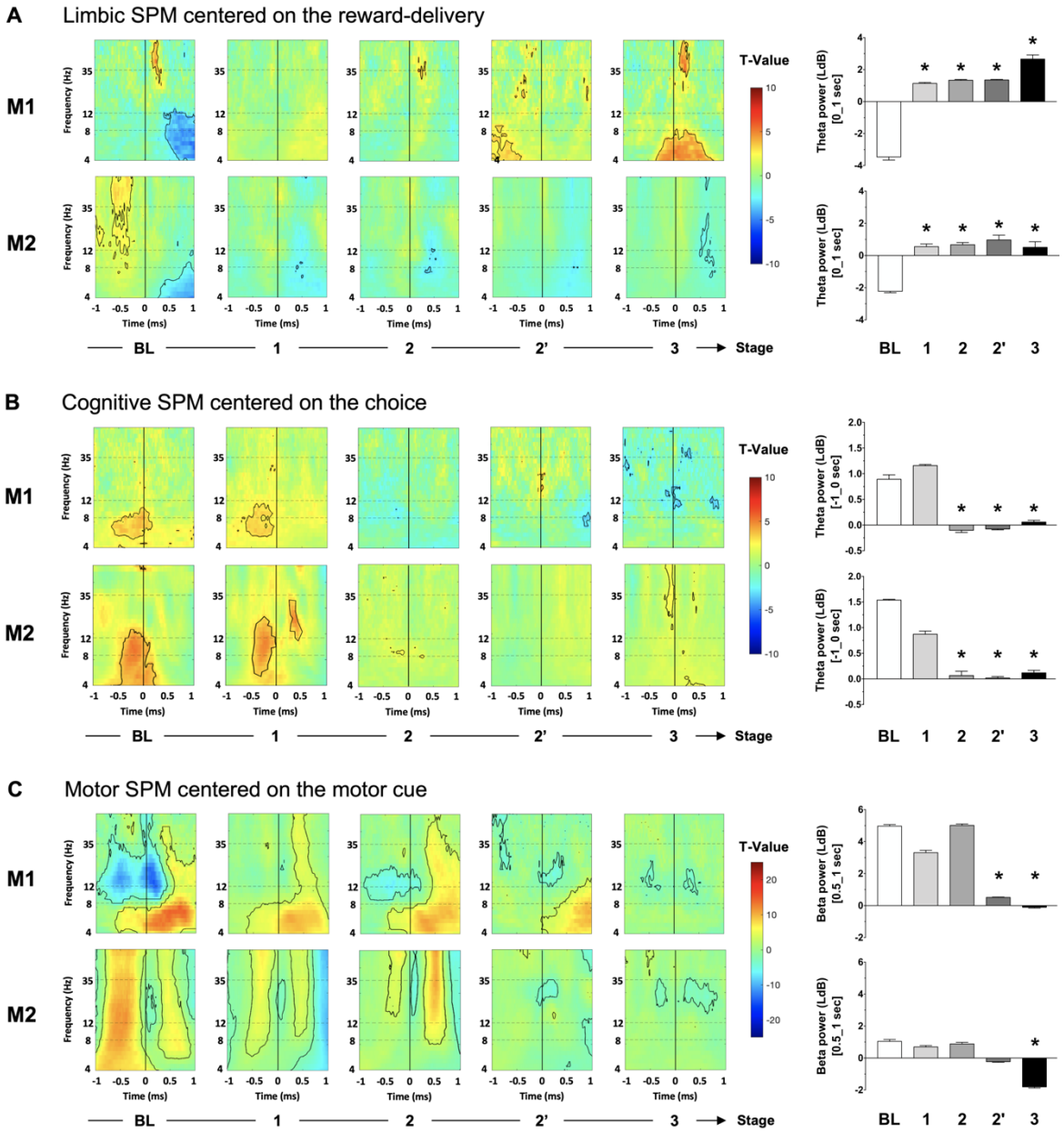

Figure 3: STN neuronal effect of MPTP treatment across stages. (A) Limbic statistical parametric maps (SPM) centered on the full gauge with reward delivery (vertical line at 0) relative to the gauge view without the reward with theta quantification between 0 and 1 second. **(B)** Cognitive SPM centered on cognitive choice (vertical line at 0) to work relative to check with theta quantification between -1 and 0 second. **(C)** Motor SPM centered on the onset of Non-Switch stimulus (vertical line at 0) relative to a resting state, with beta quantification between 0.5 and 1 second. Stages: baseline, before MPTP treatment (BL); 1, asymptomatic; 2, early mild parkinsonism; 2', late mild parkinsonism, 3, moderate parkinsonism. Significant values are encircled with solid lines $p<0.05$. Power quantifications are expressed in LdB with mean ± SEM, and *$p<0.05$.

STN modulation on parkinsonian syndrome

In stage 3, when both monkeys exhibited a stable moderate parkinsonian syndrome, LFS (4 Hz) and HFS (130 Hz) were applied to the ventral and dorsal STN. Each animal completed at least five sessions per condition (≥4 bonus rewards/session; **Supplemental Table 2**). Despite inter-

individual variability, consistent with PD patients reports [32], both monkeys showed converging effects.

Ventral LFS-STN restored the decreased motivation (Check Reward) to baseline value (for **M1-** MPTP ventral LFS: 27% (IQR 24-27) vs. MPTP: 17% (16-24) p=0.049 and BL: 28% (24-32), p=0.999; for **M2-** MPTP ventral LFS: 22% (21-25) vs. MPTP: 16% (14-19) p=0.044 and BL: 23% (21-27), p=0.998) (**Fig. 4A**).

Errors on Switch trials were almost eliminated with both LFS and HFS, regardless of dorsal or ventral STN stimulation (for **M1-** MPTP: 8.4% (IQR 8.2-8.7) vs. MPTP ventral LFS: 0.29% (0.09-0.65); MPTP dorsal LFS: 0.06% (0.04-0.08); MPTP ventral HFS: 0.07% (0.03-0.09); MPTP dorsal HFS: 0.06% (0.03-0.06), p<0.001; for **M2-** MPTP: 7.4% (7.1-8.5) vs. MPTP ventral LFS: 0.04% (0.04-0.05); MPTP dorsal LFS: 0.07% (0.04-0.08); MPTP ventral HFS: 0.14% (0.11-0.15); MPTP dorsal HFS: 0.06 (0.06-0.08), p<0.001) (**Fig. 4B**).

In contrast, dorsal LFS-STN increased Switch-Cost compared to both baseline and MPTP (for **M1-** MPTP dorsal LFS: 63.5 ± 3.4ms vs. MPTP: -10.6 ± 4.1ms and BL: 37.0 ± 1.8ms, p<0.001; for **M2-** MPTP dorsal LFS: 116.0 ± 4.3ms vs. MPTP: -40.3 ± 10.6ms and BL: 45.1 ± 1.5, p<0.001) (**Fig. 4C**).

Finally, only dorsal HFS-STN restored the mRT to baseline value (for **M1-** MPTP dorsal HFS: 388ms (IQR 347-460) vs. MPTP: 501ms (460-603), p<0.001 and BL: 411 (372-478), p>0.999; for **M2-** MPTP dorsal HFS: 435ms (378-534) vs. MPTP: 487ms (399-676), p<0.001 and BL: 454ms (390-536), p>0.999) (**Fig. 4D**).

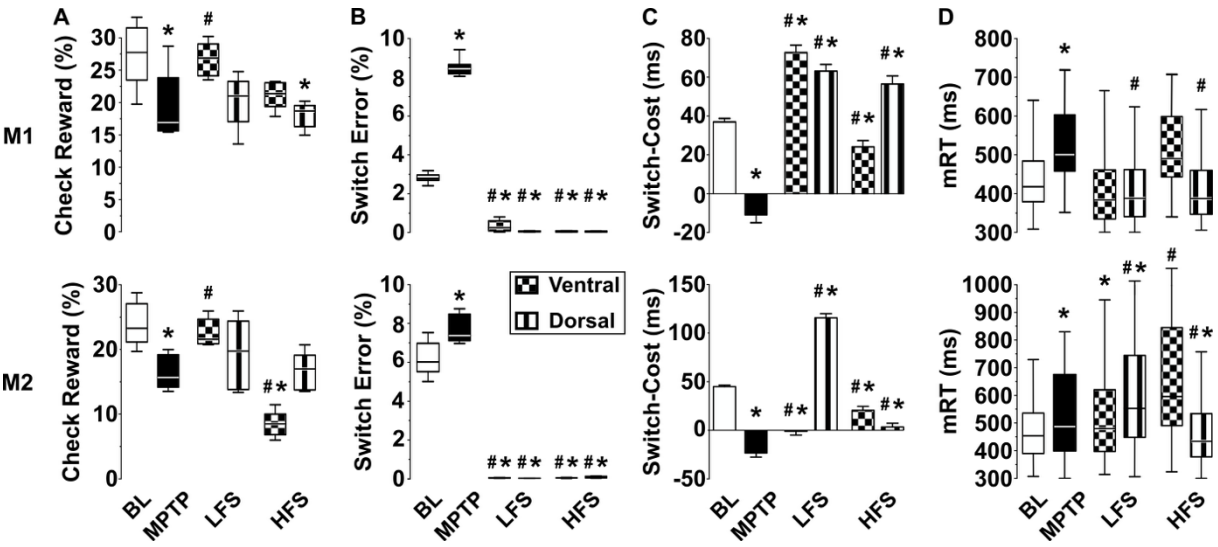

Figure 4: Behavioral effect of LFS (4Hz) and HFS (130Hz) on ventral (grid pattern) and dorsal (vertical lines) STN, on MPTP-treated monkeys. (A) Probabilities to check when the reward is available (Check Reward, %). **(B)** Errors on Switch trials (Switch Error, %). **(C)** Switch-Cost in ms, response time difference between Switch and Non-Switch trials. **(D)** Motor response time (mRT, ms). BL, baseline (white); MPTP, stage 3 (black); LFS, 4 Hz applied in stage 3; HFS, 130 Hz applied in stage

3. The horizontal line represents the median, except for Switch-Cost (mean ± SEM). *p<0.05 different from baseline and #p<0.05 different from MPTP off-stimulation, Kruskal-Wallis followed by Dunn's multiple comparisons test.

DISCUSSION

Using chronic low-dose MPTP to develop a progressive PD model, we demonstrated that non-motor impairments emerge prior to motor signs and that these behavioral changes correlate with early alterations in STN activity. In stable parkinsonism, we further show a novel positive effect of ventral LFS-STN in alleviating motivational deficits, while confirming the efficacy of dorsal HFS-STN in managing motor impairments, underscoring the site and frequency-specific contributions of STN circuits to both motor and non-motor outcomes.

Progressive parkinsonian syndrome

Among NHP models, MPTP uniquely reproduces a comprehensive nigrostriatal dopamine deficit[17], with human-like clinical features including motor symptoms, sleep/wake disturbances, and cognitive impairments[20,31,33]. In our progressive model, both monkeys developed a months-long worsening parkinsonian syndrome, mirroring the slow progression of human PD and allowing severity-stage discrimination consistent with previous studies. Interestingly, we observed a transient increase in striatal presynaptic dopamine reuptake for M1 during mild parkinsonism. Such fluctuations are consistent with preclinical and clinical observations[36–38], where increased dopamine synthesis and turnover, as well as downregulation of DaT density, likely contribute to compensatory mechanisms during the prodromal stage.

We also observed CSF decreases in HVA, MHGP, and 5-HIAA, indicating impaired dopamine, noradrenergic and serotonin neurotransmission, patterns reported across PD models and patients[42–44], and correlating with movement disorders, depression, impulsivity, and cognitive impairments[42,45–47].

Behavioral impairments follow STN activity changes

In line with recent studies linking neural activity to PD symptoms severity[48–50], we demonstrated that alterations in STN activity precede behavioral changes in a defined temporal sequence (motivational, followed by cognitive, and ultimately motor deficits), thereby defining parkinsonian stages **(Fig. 5)**.

The first stage, after first MPTP injections, is characterized by the absence of significant behavioral changes and therefore considered asymptomatic. In parallel, we observed a baseline-related decrease in theta oscillations during reward delivery, which disappeared from this stage

forward. STN theta activity has been associated with limbic processes: in parkinsonian rats as a predictor of addiction vulnerability[51], and in PD patients with emotional voice processing[52], reward and loss anticipation[12], pathological gambling[53], and depressive symptoms[13]. Notably, an EEG study reported that apathetic PD patients displayed higher baseline alpha-theta power than non-apathetic patients, suggesting that elevated alpha-theta activity may interfere with the neural dynamics required for incentivized movements[54].

Early stage 2 was defined by reduced motivation, resembling apathy reported in PD models[55,56] and PD patients[57]. In parallel, decision-related STN theta activity disappeared from this stage onward, consistent with the role of prefrontal-STN circuit in deliberative action selection during a conflict state[11,58]. Additionally, studies have shown that increased STN theta-alpha power is associated with decision-making and conflict resolution[59,60], whereas a decrease is associated with impulse control deficits and obsessive-compulsive disorder[61,62].

Late stage 2' was characterized by cognitive deficits resembling PD mild cognitive impairment[63–65]. Interestingly, both error rate and switch-cost were impacted for M2, whereas only error rate increased for M1, consistent with the transient striatal DaT increase and potential compensatory mechanisms previously discussed. In parallel, movement-related beta dynamics changed: the characteristic movement pattern of beta desynchronization followed by a rebound[66] was lost from this stage onward. Increased STN beta activity is a validated biomarker in PD and scales with motor symptoms severity[10,67–70]. We therefore hypothesize that motor beta activity variations are flattened by the overall beta increase as parkinsonism progresses.

In stage 3, in addition to motivational and cognitive deficits, clear motor manifestations appeared. These observations are consistent with the course of PD, in which non-motor symptoms precede motor symptoms by several years[2,47].

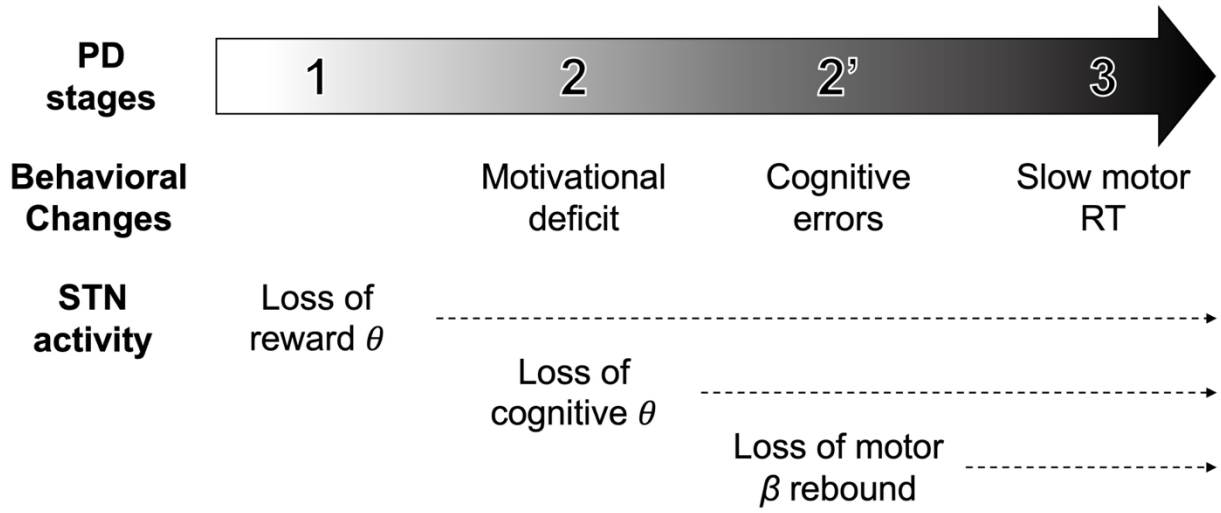

Figure 5: Study-based correlation between subthalamic nucleus (STN) alterations and the subsequent emergence of behavioral changes in a progressive model of Parkinson's disease (PD). Chronic low-dose MPTP induced distinct stages: 1, asymptomatic; 2, mild parkinsonism with motivational deficits; 2', novel intermediate stage with cognitive impairments; and 3: moderate parkinsonism with significant motor signs. RT, response time; θ, theta activity; β, beta activity.

STN modulation

STN-DBS remains the main symptomatic surgical treatment in PD, typically with HFS (130 Hz) targeting dorsolateral STN[7]. Alternative paradigms have been investigated, with dorsal LFS (4-5 Hz) showing promising cognitive improvement[24,25]. Based on these findings, we tested both HFS and LFS in dorsal and ventral STN. Despite inter-individual variability, consistent with clinical reports[27,32], we observed converging site and frequency-specific effects.

As expected, HFS in dorsal STN improved motor impairments. However, when applied in ventral STN, it aggravated motivational deficits for M2, mirroring the exacerbation of apathy and mood disturbances reported in some PD patients after DBS surgery[22].

Conversely, LFS in dorsal STN increased the Switch-Cost, consistent with previous 4 Hz STN-DBS findings showing improved inhibition of impulsive/premature responses by engaging prefrontal-STN circuits[24].

Most strikingly, we found for the first time that ventral LFS restored parkinsonian motivational deficits to baseline levels. This aligns with clinical observations where stimulation closer to the ventral STN is associated with greater improvements in anxiety and depression symptoms[71]; although ventral 4 Hz-LFS was not explored[72].

Limitations

While our parkinsonian model offers strong translational value by reproducing a progressive syndrome with both motor and non-motor clinical features, the underlying degenerative mechanisms differ between MPTP toxicity and human PD. Numerous studies have discussed strengths and limitations of this model, most notably the lack of Lewy bodies, a hallmark of alpha-synucleinopathies[17,73–75].

Another limitation is the small sample size, inherent to NHP research where ethical and logistical constraints preclude large cohorts[76,77]. Nevertheless, intra-individual longitudinal comparisons across parkinsonian stages are a strength of preclinical studies, inaccessible in human research. Finally, variability in STN recording and stimulation sites between the two monkeys may have contributed to inter-individual discrepancies, similar to clinical DBS where subtle differences in lead location strongly influence behavioral outcomes[78,79].

Conclusion

Our findings demonstrate that progressive dopamine depletion reshapes STN functional activity in a way that predicts the emergence of non-motor and motor manifestations. Motivational and cognitive impairments should therefore be expected early in PD and actively assessed with appropriate clinical evaluations. Furthermore, the site and frequency-specific effects of ventral LFS and dorsal HFS highlight the therapeutic potential of adaptive DBS strategies, offering a promising approach to manage both motor and non-motor symptoms in PD.

MATERIAL AND METHODS

Animals

This study involved two 8 years old monkeys (*Macaca fascicularis*, CRP, Port Louis, Mauritius), one male (M1, 9 kg) and one female (M2, 4 kg). They were pair-housed in a temperature (22 ± 1°C) and humidity (50 ± 5%) controlled facility with a 12h light-dark cycle. They had free access to primate chow and water, and supplemental fruits were given once a day. All procedures followed the European Communities Council Directive of 2010 (2010/63/UE) for care of laboratory animals with the recommendations of the French National Committee (2013/113) and were approved by the local Ethical Committee (#04; authorization n°2019013116115695).

Experimental design

Behavioral task. Monkeys performed a counter-demanding task assessing limbic, cognitive and motor behaviors, as previously described [16]. Animals were habituated to a primate chair (Crist Instrument Co., MD, USA) and interacted with a touch screen (Elo Touch Solutions, Inc.). In each trial, they chose either to Work on rewarded switching task (triangle, upper center) or to Check their progress with a gauge indicting the proximity of a bonus reward (cross, bottom center). When selecting Work, a blue square (Non-Switch) or an orange star (Switch) appeared randomly left or right and monkeys had to touch the blue square directly or the opposite side of the orange star. Non-Switch trials occurred with higher probability (80%) than Switch trials (20%). Correct responses within 2000 ms were rewarded (sweet liquid, 1 ml) by a computer-controlled system (Crist Instrument Co.), and each trial ended with a 1000 ms red circle before the next Work/Check choice. In Check trials, a gauge (large green circle) was displayed for 5000 ms, filling proportionally with correct Work responses (randomly 8, 16, 24, or 32 required). When Checking a full gauge, a bonus reward (sweet liquid, 5 ml) was delivered, after which the gauge reset. Incorrect responses did not affect the gauge.

Behavioral analyses. Only sessions with more than four earned bonus rewards were included. Response times (RT, time between the appearance and touch of the stimulus) were measured from correct trials: motor RT (mRT, motor behavior) for Non-Switch trials and cognitive RT (cRT) for Switch trials. Differences between cRT and mRT represented the Switch-Cost (cognitive behavior). Error rate on Switch trials (cognitive behavior) and probabilities to Check when the gauge was full (Reward Check, limbic behavior) were calculated.

Parkinsonian syndrome

MPTP treatment. Monkeys were chronically intoxicated with biweekly intramuscular 1-methyl-4-phenyl-1,2,3,6-tetrahydropyridine (MPTP) injections (0.2-0.5 mg/kg, in NaCl 0.9%) under light anesthesia (Ketamine 2-4 mg/kg), as previously described [31]. After each injection, motor score was assessed, and doses were adjusted. M1 received 20 injections over 43 weeks (5.45 mg/kg total) and M2 received 18 injections over 39 weeks (6.7 mg/kg total). Both exhibited a similar stable parkinsonian syndrome.

Motor score. Behavioral evaluation was performed, throughout MPTP treatment in the home cage, using a validated macaque parkinsonism scale (Imbert et al., 2000; Davin et al., 2022). Eight criteria were scored from 0 (no impairment) to 3 (maximal impairment), including each arm movement frequency, general activity, posture, bradykinesia, tremor, feeding, freezing and vocalizations (**Supplemental Fig. 1**). According to the literature, three severity stages were identified: stage 1, asymptomatic (0-3); stage 2, mild parkinsonism (4-10); and stage 3, moderate parkinsonism without care needed (>10) (Devergnas et al., 2014; Davin et al., 2022).

DaT SPECT imaging. Striatal dopaminergic system was assessed at baseline and across parkinsonian stages using Ioflupane tracer (I123, 90 MBq), which binds to presynaptic dopamine transporters (DaT). For all exams, monkeys were anesthetized for intravenous tracer injection, and images were acquired 3 hours later. A zoom lens was applied for M2 due to sexual dimorphism. Semi-quantitative analysis of striatal ROI was calculated from the three slices with maximal radioactivity and normalized to an occipital cortex ROI.

CSF analysis. At baseline and throughout MPTP treatment, CSF was collected under anesthesia by lumbar puncture (L4/L5) using a 22 g Quincke spinal needle (BD™). Sample were stored on ice in sterile 1.5 mL polypropylene tubes, and frozen at -80°C. Monoaminergic

metabolites (homovanillic acid, HVA; 5-hydroxyindole acetic acid, 5-HIAA; 3-methoxy-4-hydroxyphenylglycol, MHPG; and 3-orthomethyl-DOPA, 3-OMD), were quantified by ion pair high performance liquid chromatography with electrochemical detection, as previously described [81].

Surgical procedure

Electrode implantation was performed under aseptic conditions and general anesthesia, as previously described [16]. Monkeys were initially anesthetized with ketamine (7 mg/kg) and xylazine (0.6 mg/kg), and maintained anesthetized with isoflurane. Lidocaine 1% was used for local anesthesia. Saline solution (NaCl 0.9%, Sigma-Aldrich) was infused intravenously during surgery for drug access and hydration. Pre-operative 7T MRI (IRMaGE, Grenoble) allowed the STN identification and per-operative X-rays with ventriculography localized the anterior and posterior commissures (ACPC), with 2ml injection of contrast agent (Iopamiron 200, iodine 200 mg/ml, Bracc) into the left lateral ventricle. STN borders were refined using micro-recordings (250 µm diameter, 0.8-1.2 MOhm, FHC), based on firing rate and pattern. The right STN was implanted with a quadripolar DBS electrode (0.8 mm diameter, four 0.5 mm contacts in two rows, 0.5 mm apart, and and two columns; Heraus©, USA), allowing recordings and two-level stimulations. Electrode was placed at the following stereotactic coordinates: anterior 6/12th of ACPC, 4–5 mm from the midline, with deepest contacts at the lower STN border. The implantation was confirmed by radiography and ventriculography (see [16], **Fig. 1D-E**), and the reference fixed at the left occipital level. A stainless-steel head holder (Crist Instruments, MD) was placed at the back of the skull to maintain the head. Post-operative analgesic/anti-inflammatory therapy (Ketoprofen 2mg/kg) were administrated for one week.

STN recording

Baseline recordings began 2 weeks after surgery and continue throughout MPTP treatment, using a common occipital reference and a multichannel system (AlphaOmega Engineering, Israel). Signals were sampled at 1375 Hz, aligned to task events (± 1000 ms) and analyzed using MATLAB and ImaGIN toolbox (MathWorks). Time-frequency representations of spectral power (2-200 Hz) were computed using a multitaper sliding window with orthogonal discrete prolate Slepian spheroidal (DPSS) tapers, adapted to the frequency and sliding-window length. Single-trial power spectra were averaged by condition and normalized to a pre-stimulus baseline (-1000 to -250 ms) using the formula $LdB = 10 \log_{10} (P/B)$, where P is peristimulus

power and B is baseline power. Data are expressed in LdB (mean ± SEM) for specific frequency bands defined as theta (4-8 Hz), alpha (8-12 Hz), beta (12-35 Hz), and gamma (35-200 Hz).

STN stimulation

After MPTP treatment, continuous bipolar stimulation was applied in ventral or dorsal STN, at low frequency stimulation (LFS, 4 Hz), shown to improve cognitive deficits in PD patients [24,25], and high-frequency stimulation (HFS, 130 Hz), clinical standard for PD motor symptoms [7]. For each frequency, stimulation ranges were conducted until side effects occurred (e.g., ipsilateral monocular deviation, head rotation, lip contraction), and intensities set at 80% of this threshold (0.08-0.2 mA; pulse width 60 µs). The number of trials per condition is detailed in **Supplemental Table 2**.

Statistical analyses

Behavioral data. Statistical analyses were performed with GraphPad Prism 8 (GraphPad Software Inc., USA). After normality testing with Shapiro-Wilk test, Kruskal-Wallis tests, followed by Dunn's multiple comparisons tests, were applied for all behavioral data (mRT, cRT; Switch-Cost, Check Reward), enabling comparison across stages (**Supplemental Table 1**) and stimulation conditions (**Supplemental Table 2**). Data are presented as median (IQR), except for Switch-Cost (mean ± SEM), and a difference was considered statistically significant for a value of $p < 0.05$.

Statistical parametric maps. Post-hoc t-tests for time-frequency representations of spectral power were Bonferroni corrected, with "one-sample" t-test to compare signal of one event, and "two-sample" t-test to discriminate significant differences between two events (T-Values). These analyses were plotted as statistical parametric maps (SPM) with significant value encircled ($p < 0.05$). For band-specific analyses, mean relative power were compared across stages using ANOVA followed by Tukey's test. Data are presented as mean ± SEM and a difference was considered statistically significant for a value of $p < 0.05$.

Acknowledgements

This work was supported by the French Agence Nationale de la Recherche (ANR), under grant ANR-18-BS01-0005.

Conflict of interest

The authors declare no competing financial interests related to this work.

Data Availability

Data and code are available from the corresponding author upon request.

REFERENCES

1. Chaudhuri, K. R. *et al.* The nondeclaration of nonmotor symptoms of Parkinson's disease to health care professionals: An international study using the nonmotor symptoms questionnaire. *Movement Disorders* **25**, 704–709 (2010).
2. Poewe, W. Non-motor symptoms in Parkinson's disease. *Euro J of Neurology* **15**, 14–20 (2008).
3. Weintraub, D. *et al.* The neuropsychiatry of Parkinson's disease: advances and challenges. *The Lancet Neurology* **21**, 89–102 (2022).
4. Tolosa, E., Garrido, A., Scholz, S. W. & Poewe, W. Challenges in the diagnosis of Parkinson's disease. *The Lancet Neurology* **20**, 385–397 (2021).
5. Hamani, C. The subthalamic nucleus in the context of movement disorders. *Brain* **127**, 4–20 (2004).
6. Haynes, W. I. A. & Haber, S. N. The Organization of Prefrontal-Subthalamic Inputs in Primates Provides an Anatomical Substrate for Both Functional Specificity and Integration: Implications for Basal Ganglia Models and Deep Brain Stimulation. *J. Neurosci.* **33**, 4804–4814 (2013).
7. Benabid, A. L., Chabardes, S., Mitrofanis, J. & Pollak, P. Deep brain stimulation of the subthalamic nucleus for the treatment of Parkinson's disease. **8**, (2009).
8. Bergman, H., Wichmann, T., Karmon, B. & DeLong, M. R. The primate subthalamic nucleus. II. Neuronal activity in the MPTP model of parkinsonism. *Journal of Neurophysiology* **72**, 507–520 (1994).

9. Eusebio, A. *et al.* Deep brain stimulation can suppress pathological synchronisation in parkinsonian patients. *Journal of Neurology, Neurosurgery & Psychiatry* **82**, 569–573 (2011).
10. Neumann, W. *et al.* Subthalamic synchronized oscillatory activity correlates with motor impairment in patients with Parkinson's disease. *Movement Disorders* **31**, 1748–1751 (2016).
11. Cavanagh, J. F. *et al.* Subthalamic nucleus stimulation reverses mediofrontal influence over decision threshold. *Nat Neurosci* **14**, 1462–1467 (2011).
12. Manssuer, L. *et al.* Subthalamic Oscillatory Activity of Reward and Loss Processing Using the Monetary Incentive Delay Task in Parkinson Disease. *Neuromodulation: Technology at the Neural Interface* **26**, 414–423 (2023).
13. Sun, Y. *et al.* α and θ oscillations in the subthalamic nucleus are potential biomarkers for Parkinson's disease with depressive symptoms. *Parkinsonism & Related Disorders* **90**, 98–104 (2021).
14. Wang, Y. *et al.* Subthalamic stimulation causally modulates human voluntary decision-making to stay or go. *npj Parkinsons Dis.* **10**, 210 (2024).
15. Zavala, B., Zaghloul, K. & Brown, P. The subthalamic nucleus, oscillations, and conflict. *Movement Disorders* **30**, 328–338 (2015).
16. Bertrand, M. *et al.* Contribution of the subthalamic nucleus to motor, cognitive and limbic processes: an electrophysiological and stimulation study in monkeys. *Front. Neurosci.* **18**, 1257579 (2024).
17. Bezard, E. *et al.* Position paper: leveraging non-human primate (NHP) specificities to accelerate Parkinson's disease and ageing research. *npj Parkinsons Dis.* **11**, 227 (2025).

18. Burns, R. S. *et al.* A primate model of parkinsonism: selective destruction of dopaminergic neurons in the pars compacta of the substantia nigra by N-methyl-4-phenyl-1,2,3,6-tetrahydropyridine. *Proc. Natl. Acad. Sci. U.S.A.* **80**, 4546–4550 (1983).
19. Masilamoni, G. J., Weinkle, A., Papa, S. M. & Smith, Y. Cortical Serotonergic and Catecholaminergic Denervation in MPTP-Treated Parkinsonian Monkeys. *Cerebral Cortex* **32**, 1804–1822 (2022).
20. Schneider, J. S. & Kovelowski, C. J. Chronic exposure to low doses of MPTP. I. Cognitive deficits in motor asymptomatic monkeys. *Brain Research* **519**, 122–128 (1990).
21. Seo, J. *et al.* A non-human primate model for stable chronic Parkinson's disease induced by MPTP administration based on individual behavioral quantification. *Journal of Neuroscience Methods* **311**, 277–287 (2019).
22. Kurtis, M. M., Rajah, T., Delgado, L. F. & Dafsari, H. S. The effect of deep brain stimulation on the non-motor symptoms of Parkinson's disease: a critical review of the current evidence. *npj Parkinson's Disease* **3**, 16024 (2017).
23. Temel, Y. *et al.* Behavioural changes after bilateral subthalamic stimulation in advanced Parkinson disease: A systematic review. *Parkinsonism & Related Disorders* **12**, 265–272 (2006).
24. Kelley, R. *et al.* A human prefrontal-subthalamic circuit for cognitive control. *Brain* **141**, 205–216 (2018).
25. Qin, G. *et al.* Unlocking potential: low frequency subthalamic nucleus stimulation enhances executive function in Parkinson's disease patients with postural instability/gait disturbance. *Front. Neurosci.* **17**, 1228711 (2023).
26. Singh, A. *et al.* Frontal theta and beta oscillations during lower-limb movement in Parkinson's disease. *Clinical Neurophysiology* **131**, 694–702 (2020).

27. Busch, J. L. *et al.* Chronic adaptive deep brain stimulation for Parkinson's disease: clinical outcomes and programming strategies. *npj Parkinsons Dis.* **11**, 264 (2025).
28. Horn, A. & Neumann, W.-J. From adaptive deep brain stimulation to adaptive circuit targeting. *Nat Rev Neurol* https://doi.org/10.1038/s41582-025-01131-5 (2025) doi:10.1038/s41582-025-01131-5.
29. Little, S. *et al.* Bilateral adaptive deep brain stimulation is effective in Parkinson's disease. *J Neurol Neurosurg Psychiatry* **87**, 717–721 (2016).
30. Tinkhauser, G. *et al.* The modulatory effect of adaptive deep brain stimulation on beta bursts in Parkinson's disease. *Brain* **140**, 1053–1067 (2017).
31. Davin, A. *et al.* Early onset of sleep/wake disturbances in a progressive macaque model of Parkinson's disease. *Sci Rep* **12**, 17499 (2022).
32. Rossi, M., Bruno, V., Arena, J., Cammarota, Á. & Merello, M. Challenges in PD Patient Management After DBS: A Pragmatic Review. *Movement Disord Clin Pract* **5**, 246–254 (2018).
33. Porras, G., Li, Q. & Bezard, E. Modeling Parkinson's Disease in Primates: The MPTP Model. *Cold Spring Harbor Perspectives in Medicine* **2**, a009308–a009308 (2012).
34. Connolly, A. T. *et al.* Modulations in Oscillatory Frequency and Coupling in Globus Pallidus with Increasing Parkinsonian Severity. *J. Neurosci.* **35**, 6231–6240 (2015).
35. Devergnas, A., Pittard, D., Bliwise, D. & Wichmann, T. Relationship between oscillatory activity in the cortico-basal ganglia network and parkinsonism in MPTP-treated monkeys. *Neurobiology of Disease* **68**, 156–166 (2014).
36. Appel-Cresswell, S., De La Fuente-Fernandez, R., Galley, S. & McKeown, M. J. Imaging of compensatory mechanisms in Parkinson's disease. *Current Opinion in Neurology* **23**, 407–412 (2010).

37. Boulet, S. *et al.* Behavioral Recovery in MPTP-Treated Monkeys: Neurochemical Mechanisms Studied by Intrastriatal Microdialysis. *J. Neurosci.* **28**, 9575–9584 (2008).
38. Senior, S. L. *et al.* Increased striatal dopamine release and hyperdopaminergic-like behaviour in mice lacking both alpha-synuclein and gamma-synuclein. *Eur J of Neuroscience* **27**, 947–957 (2008).
39. Mounayar, S. *et al.* A new model to study compensatory mechanisms in MPTP-treated monkeys exhibiting recovery. *Brain* **130**, 2898–2914 (2007).
40. Vezoli, J. *et al.* Early Presymptomatic and Long-Term Changes of Rest Activity Cycles and Cognitive Behavior in a MPTP-Monkey Model of Parkinson's Disease. *PLOS ONE* **6**, e23952 (2011).
41. Vezoli, J. *et al.* Increased DAT binding in the early stage of the dopaminergic lesion: A longitudinal [11C]PE2I binding study in the MPTP-monkey. *NeuroImage* **102**, 249–261 (2014).
42. Barone, P. Neurotransmission in Parkinson's disease: beyond dopamine. *Euro J of Neurology* **17**, 364–376 (2010).
43. Masilamoni, G. J. & Smith, Y. Chronic MPTP administration regimen in monkeys: a model of dopaminergic and non-dopaminergic cell loss in Parkinson's disease. *J Neural Transm* **125**, 337–363 (2018).
44. Wihan, J. *et al.* Layer-specific axonal degeneration of serotonergic fibers in the prefrontal cortex of aged A53T α-synuclein–expressing mice. *Neurobiology of Aging* **80**, 29–37 (2019).
45. Brown, G. L. & Linnoila, M. I. CSF serotonin metabolite (5-HIAA) studies in depression, impulsivity, and violence. *The Journal of Clinical Psychiatry* **51**, 31–41 (1990).
46. Cooper, S. J., King, D. J. & Kelly, C. B. 5-hydroxyindoleacetic acid in cerebrospinal fluid and prediction of suicidal behaviour in schizophrenia. *The Lancet* **340**, 940–941 (1992).

47. Schapira, A. H. V., Chaudhuri, K. R. & Jenner, P. Non-motor features of Parkinson disease. *Nat Rev Neurosci* **18**, 435–450 (2017).

48. Hassin-Baer, S. *et al.* Identification of an early-stage Parkinson's disease neuromarker using event-related potentials, brain network analytics and machine-learning. *PLoS ONE* **17**, e0261947 (2022).

49. Lee, L.-H. N. *et al.* An electrophysiological perspective on Parkinson's disease: symptomatic pathogenesis and therapeutic approaches. *J Biomed Sci* **28**, 85 (2021).

50. Wang, L. *et al.* Association of Structural Measurements of Brain Reserve With Motor Progression in Patients With Parkinson Disease. *Neurology* **99**, (2022).

51. Degoulet, M., Tiran-Cappello, A., Combrisson, E., Baunez, C. & Pelloux, Y. Subthalamic low-frequency oscillations predict vulnerability to cocaine addiction. *Proc. Natl. Acad. Sci. U.S.A.* **118**, e2024121118 (2021).

52. Benis, D. *et al.* Subthalamic nucleus oscillations during vocal emotion processing are dependent of the motor asymmetry of Parkinson's disease. *NeuroImage* **222**, 117215 (2020).

53. Rosa, M. *et al.* Pathological gambling in Parkinson's disease: Subthalamic oscillations during economics decisions. *Movement Disorders* **28**, 1644–1652 (2013).

54. Zhu, M. *et al.* Altered EEG alpha and theta oscillations characterize apathy in Parkinson's disease during incentivized movement. *NeuroImage: Clinical* **23**, 101922 (2019).

55. Brown, C. A. *et al.* Dopamine pathway loss in nucleus accumbens and ventral tegmental area predicts apathetic behavior in MPTP-lesioned monkeys. *Experimental Neurology* **236**, 190–197 (2012).

56. Magnard, R. *et al.* What can rodent models tell us about apathy and associated neuropsychiatric symptoms in Parkinson's disease? *Transl Psychiatry* **6**, e753–e753 (2016).

57. Den Brok, M. G. H. E. *et al.* Apathy in Parkinson's disease: A systematic review and meta-analysis. *Movement Disorders* **30**, 759–769 (2015).
58. Alegre, M. *et al.* The subthalamic nucleus is involved in successful inhibition in the stop-signal task: A local field potential study in Parkinson's disease. *Experimental Neurology* **239**, 1–12 (2013).
59. Fumagalli, M. *et al.* Conflict-dependent dynamic of subthalamic nucleus oscillations during moral decisions. *Social Neuroscience* **6**, 243–256 (2011).
60. Zénon, A. *et al.* The human subthalamic nucleus encodes the subjective value of reward and the cost of effort during decision-making. *Brain* **139**, 1830–1843 (2016).
61. Bastin, J. *et al.* Changes of oscillatory activity in the subthalamic nucleus during obsessive-compulsive disorder symptoms: Two case reports. *Cortex* **60**, 145–150 (2014).
62. Rodriguez-Oroz, M. C. *et al.* Involvement of the subthalamic nucleus in impulse control disorders associated with Parkinson's disease. *Brain* **134**, 36–49 (2011).
63. Aarsland, D. *et al.* Range of neuropsychiatric disturbances in patients with Parkinson's disease. *Journal of Neurology, Neurosurgery & Psychiatry* **67**, 492–496 (1999).
64. Cammisuli, D. M., Cammisuli, S. M., Fusi, J., Franzoni, F. & Pruneti, C. Parkinson's Disease–Mild Cognitive Impairment (PD-MCI): A Useful Summary of Update Knowledge. *Front. Aging Neurosci.* **11**, 303 (2019).
65. Goldman, J. & Litvan, I. Mild Cognitive Impairment in Parkinson's Disease. (2012).
66. Pfurtscheller, G. & Lopes Da Silva, F. H. Event-related EEG/MEG synchronization and desynchronization: basic principles. *Clinical Neurophysiology* **110**, 1842–1857 (1999).
67. Bharti, E. *et al.* Alterations in beta oscillatory activity occur with the emergence of parkinsonian motor signs across the basal ganglia-thalamocortical network. *Neurobiology of Disease* **215**, 107075 (2025).

68. Deffains, M., Iskhakova, L., Katabi, S., Israel, Z. & Bergman, H. Longer β oscillatory episodes reliably identify pathological subthalamic activity in Parkinsonism. *Movement Disorders* **33**, 1609–1618 (2018).
69. Lofredi, R. *et al.* Beta bursts during continuous movements accompany the velocity decrement in Parkinson's disease patients. *Neurobiology of Disease* **127**, 462–471 (2019).
70. Tinkhauser, G. *et al.* Beta burst coupling across the motor circuit in Parkinson's disease. *Neurobiology of Disease* **117**, 217–225 (2018).
71. Zhang, F. *et al.* Correlation between Electrode Location and Anxiety Depression of Subthalamic Nucleus Deep Brain Stimulation in Parkinson's Disease. *Brain Sciences* **12**, 755 (2022).
72. Mann, G. S. *et al.* Comparing the impact of low frequency vs high frequency deep brain stimulation in Patient's with Parkinson's disease: A systematic review. *Brain Disorders* **19**, 100239 (2025).
73. AlShimemeri, S., Di Luca, D. G. & Fox, S. H. MPTP Parkinsonism and Implications for Understanding Parkinson's Disease. *Movement Disord Clin Pract* **9**, 42–47 (2022).
74. Bezard, E., Yue, Z., Kirik, D. & Spillantini, M. G. Animal models of Parkinson's disease: Limits and relevance to neuroprotection studies. *Movement Disorders* **28**, 61–70 (2013).
75. Bové, J., Prou, D., Perier, C. & Przedborski, S. Toxin-induced models of Parkinson's disease. *Neurotherapeutics* **2**, 484–494 (2005).
76. National Academies of Sciences, Engineering & Medicine. *Nonhuman Primate Models in Biomedical Research: State of the Science and Future Needs*. (The National Academies Press, Washington, DC, 2023). doi:10.17226/26857.
77. Phillips, K. A. *et al.* Why primate models matter. *American J Primatol* **76**, 801–827 (2014).

78. Liang, K. *et al.* Emotional symptoms and cognitive function outcomes of subthalamic stimulation in Parkinson's disease depend on location of active contacts and the volume of tissue activated. *CNS Neurosci Ther* **29**, 2355–2365 (2023).

79. York, M. K., Wilde, E. A., Simpson, R. & Jankovic, J. Relationship between neuropsychological outcome and DBS surgical trajectory and electrode location. *Journal of the Neurological Sciences* **287**, 159–171 (2009).

80. Imbert, C., Bezard, E., Guitraud, S., Boraud, T. & Gross, C. E. Comparison of eight clinical rating scales used for the assessment of MPTP-induced parkinsonism in the Macaque monkey. *Journal of Neuroscience Methods* **96**, 71–76 (2000).

81. Ormazabal, A. *et al.* HPLC with electrochemical and fluorescence detection procedures for the diagnosis of inborn errors of biogenic amines and pterins. *Journal of Neuroscience Methods* **142**, 153–158 (2005).